Wuthrich, K., Aviram, I., & Schejter, A. (1971) *Biochim. Biophys. Acta 253*, 98–103.
Yu, L. P., & Smith, G. M. (1988a) *Biochemistry 27*, 1949–1956.
Yu, L. P., & Smith, G. M. (1988b) *Proc. Natl. Acad. Sci. U.S.A. 85*, 2894–2898.
Yu, L. P., & Smith, G. M. (1990) *Biochemistry* (preceding paper in this issue).

Structural Studies with the Uveopathogenic Peptide M Derived from Retinal S-Antigen†

Arturo Muga,‡ Witold K. Surewicz, Patrick T. T. Wong, and Henry H. Mantsch*
Division of Chemistry, National Research Council of Canada, Ottawa, Canada K1A 0R6
Vijay K. Singh and Toshimichi Shinohara
Molecular Biology Section, National Eye Institute, National Institutes of Health, Bethesda, Maryland 20892
Received August 18, 1989; Revised Manuscript Received November 27, 1989

ABSTRACT: The 18-residue fragment of bovine S-antigen, corresponding to amino acid positions 303–320, is highly immunogenic and is known to induce experimental autoimmune uveitis. The solution conformation of this immunogenic peptide, known as peptide M, was studied by Fourier-transform infrared spectroscopy and by circular dichroism. In the pH range between approximately 4 and 9.5, peptide M has a strong tendency to form macromolecular assemblies in which it adopts an intermolecular β-sheet structure. The intermolecular β-sheets are stabilized by ionic interactions ("salt bridges") between the carboxylate groups and basic residues of the neighboring peptide molecules. These interactions can be disrupted by neutralization of either acidic (pH range below 4) or basic residues (pH range above 9.5) or by elevated hydrostatic pressure. The secondary structure of the peptide under conditions favoring the monomeric state appears to be a mixture of unordered structure and β-sheets. The present data are consistent with a recently proposed model [Sette, A., Buns, S., Colon, S., Smith, J. A., Miles, C., & Grey, H. M. (1987) *Nature 328*, 395–399], which assumes that certain immunogenic peptides adopt an extended β-type conformation in which they are "sandwiched" between the major histocompatibility complex and the T-cell receptor.

The S-antigen is a major soluble protein of the retina and pineal gland (Wacker et al., 1977) that binds to photo-excited–phosphorylated rhodopsin (Pfister et al., 1985) and is intimately involved in the visual cycle. The S-antigen is also a highly pathogenic protein, responsible for the induction of experimental autoimmune uveitis (Donoso et al., 1988) which has been characterized as a T-cell-mediated disease resulting in severe inflammation of the uveal tract, retina, and pineal gland (Mochizuki et al., 1985).

The specific region of S-antigen responsible for its pathogenicity has been recently identified (Donoso et al., 1987; Singh et al., 1988; Shinohara et al., 1988). Moreover, it has been shown that the synthetic octadecapeptide, known as peptide M, corresponding to amino acid positions 303–320 (Asp-Thr-Asn-Leu-Ala-Ser-Ser-Thr-Ile-Ile-Lys-Glu-Gly-Ile-Asp-Arg-Thr-Val) in bovine S-antigen is highly effective in inducing experimental autoimmune uveitis. Both clinically and histopathologically, the experimental autoimmune uveitis produced by the synthetic peptide is indistinguishable from the disease caused by the native S-antigen. The detailed understanding of the mode of action of peptide M may therefore provide essential clues for advancing our knowledge of autoimmune diseases. However, the molecular dynamic basis for the pathogenic action of peptide M and, in particular, the conformational properties of the peptide are still unknown.

In the present study, we have used infrared and circular dichroism spectroscopy to investigate the conformation of peptide M in solution. It is shown that the preferred conformation of the peptide in aqueous solution is β-sheet, although the detailed structural properties depend on the degree of peptide self-association.

Materials and Methods

Preparation of Peptide M. The octadecapeptide Asp-Thr-Asn-Leu-Ala-Ser-Ser-Thr-Ile-Ile-Lys-Glu-Gly-Ile-Asp-Arg-Thr-Val (peptide M) was synthesized by standard solid-phase chemistry in a commercial peptide synthesizer as described previously (Knight et al., 1988). In order to remove residual trifluoroacetic acid used in the synthesis of peptide M [the trifluoroacetate ion has a very strong infrared absorption band around 1670 cm^{-1} which interferes with the characteristic peptide bands (Surewicz & Mantsch, 1989)], the peptide was additionally purified by chromatography on an Amberlite IR-45 minicolumn. The column (5.5 × 80 mm) was preequilibrated with bidistilled water. The peptide was then applied as a solution in H_2O (5 mg/mL), followed by elution with bidistilled water, collection of fractions, and their lyophilization. About 80% of the starting material was recovered in the first 2-mL fraction. Peptide solutions at various concentrations and pH values were then prepared in D_2O buffer. The sequence and the concentration of the stock solutions of the octadecapeptide were confirmed by an amino acid analysis on a DURRUM 500 amino acid analyzer.

Infrared Spectroscopy. Infrared spectra under ambient conditions (room temperature and atmospheric pressure) were collected at a resolution of 2 cm^{-1} on a Digilab FTS-60 spectrometer equipped with a high-sensitivity deuterated triglycine sulfate detector. The samples were assembled into

† Issued as NRCC Publication No. 30574.
‡ Recipient of an FPI Fellowship from the Spanish Ministry of Education and Science.

0006-2960/90/0429-2925$02.50/0

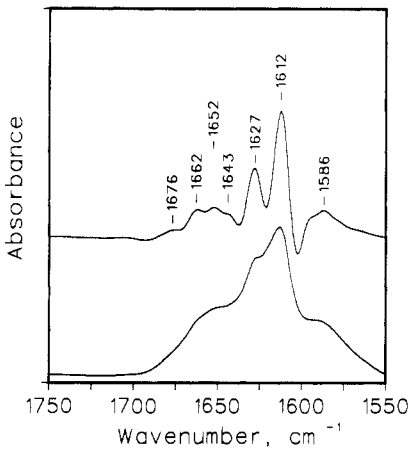

FIGURE 1: Infrared spectra in the 1500–1800-cm^{-1} region of a 5 mM solution of peptide M in 50 mM HEPES buffer in D_2O, pH 7.0. Original spectrum (bottom) and spectrum after band narrowing by Fourier self-deconvolution with a Lorentzian band of 12-cm^{-1} half-width and a k factor of 1.8 (top).

Harrick-type demountable cells fitted with CaF_2 windows and separated by a 50-μm teflon spacer. Infrared spectra at elevated hydrostatic pressure were collected at a resolution of 4 cm^{-1} on a Digilab FTS-45 spectrometer equipped with a 0.25-mm mercury–cadmium telluride detector operated at 77 K. Aqueous peptide samples (about 10 μL) were placed at room temperature in a 0.37 mm diameter hole on a diamond anvil cell, along with a few crystals of α-quartz, which was used as internal pressure calibrant (Wong et al., 1985). Band narrowing was performed according to the procedures of Fourier self-deconvolution and Fourier derivation (Moffatt et al., 1986; Mantsch et al., 1986).

Circular Dichroism. Spectra were acquired on a Jasco J600 spectropolarimeter equipped with an IBM microcomputer. Peptide solutions were placed in a 0.2 mm path length cylindrical quartz cell, and typically, eight spectra were averaged.

Results and Discussion

The usefulness of infrared spectroscopy for studying the secondary structure of proteins and polypeptides is now well recognized (Susi, 1969; Parker, 1983; Surewicz & Mantsch, 1988). The correspondence between characteristic infrared bands of proteins and the conformation of the polypeptide backbone is best understood for the amide I mode which represents primarily the stretching vibrations of the C=O groups of the protein backbone. The frequency of this vibration depends on the nature of the hydrogen bondings of the C=O groups, which, in turn, are determined by the particular secondary structure adopted by the polypeptide chains (Krimm & Bandekar, 1986).

The infrared spectrum of a 5 mM solution of the octadecapeptide at neutral pH in D_2O HEPES buffer is shown in Figure 1. The original spectrum (bottom trace) of the conformation-sensitive amide I region between 1600 and 1700 cm^{-1} exhibits a well-defined maximum at 1612 cm^{-1} and a number of pronounced shoulders which indicate that the amide I mode consists of various overlapping components. These component bands can be better visualized with Fourier self-deconvolution, a mathematical technique of band narrowing (Kauppinen et al., 1981). The spectrum after Fourier self-deconvolution (top trace) reveals, in addition to the major band at 1612 cm^{-1}, another relatively strong band at 1627 cm^{-1} and weaker bands at 1643, 1652, 1662, and 1676 cm^{-1}. The absence of an amide II band around 1550 cm^{-1} in D_2O buffer indicates that all backbone N–H groups have been deuterium exchanged. Thus, all the remaining infrared bands seen in Figure 1 are due to amino acid side-chain vibrations (Chirgadze et al., 1975).

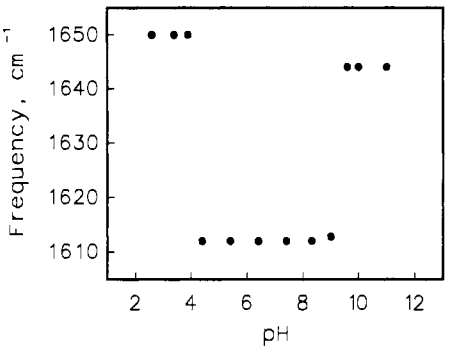

FIGURE 2: pH dependence of the frequency of the amide I band maximum of peptide M. Peptide concentration was 5 mM.

While the infrared band at 1627 cm^{-1} is highly characteristic of the peptide backbone in a β-sheet conformation, the position of the major component band at 1612 cm^{-1} is somewhat below the frequency range typical for β-sheets in globular proteins (Byler & Susi, 1986; Surewicz & Mantsch, 1988). However, bands at similar wavenumbers were observed for some synthetic peptides that form an intermolecular network of hydrogen bonded β-sheets [e.g., poly(L-lysine) at high pH (Carrier et al., 1990) or the atrial natriuretic peptide associated with lipid membranes (Surewicz et al., 1987)]. The dominance of this low-wavenumber band in the spectrum of Figure 1 strongly suggests that under the experimental conditions used (5 mM peptide solution, neutral pH) peptide M adopts an intermolecular β-sheet structure. In order to gain further insight into the forces responsible for the formation of these β-sheets, we have investigated the effect of pH, peptide concentration, and hydrostatic pressure on the conformational equilibria of peptide M in aqueous solution.

Effect of pH on Peptide M Conformation. Infrared spectra of peptide M were measured at different pH values between 2 and 11. The results of these experiments are summarized in Figure 2, which shows the position of the maximum of the amide I band contour as a function of pH. This plot clearly indicates that the octadecapeptide undergoes two conformational transitions: one at pH around 4 and one at pH around 9.5.

Infrared spectra representative of peptide M in the three different conformational states identified in Figure 2, i.e., at low pH (below 4), intermediate pH (between 4 and 9.5), and high pH (above 9.5), are illustrated in Figure 3A. The corresponding spectra after band narrowing by Fourier self-deconvolution are shown in Figure 3B.

The conformation-sensitive amide I region of the infrared spectrum of peptide M at pH >9.5 is dominated by a single band centered at around 1643 cm^{-1} (bottom trace in Figure 3B), which is highly characteristic of the peptide backbone in a nonordered conformation (Surewicz & Mantsch, 1988). There is no indication of regular ordered structures such as α-helices or β-sheets. The weak shoulder band around 1662 cm^{-1} is indicative of amino acids engaged in turns (Byler & Susi, 1986). At this pH all acid side-chain groups are ionized, and a number of characteristic side-chain bands can be seen in the infrared spectrum. The bands at 1565 and 1586 cm^{-1} represent carboxylate groups of glutamic acid and aspartic acid, respectively, while the very weak band at 1609 cm^{-1} originates from the guanidine group of arginine (Chirgadze et al., 1975). The arginine group also yields a band around 1590 cm^{-1} which overlaps with the aspartate band at 1586 cm^{-1}.

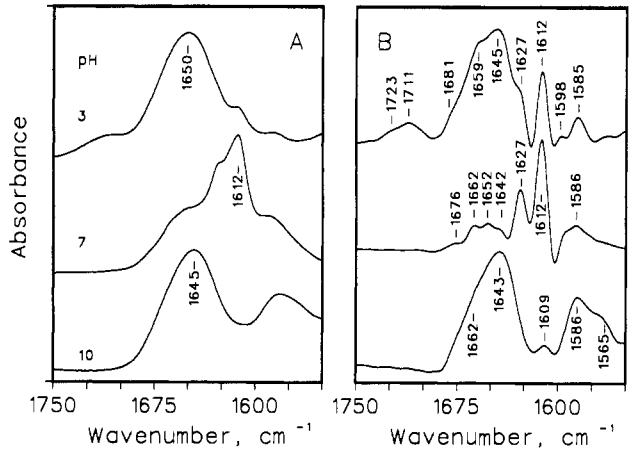

FIGURE 3: Infrared spectra in the 1550–1750-cm^{-1} region of peptide M at pH 3 (top spectra), 7 (middle spectra), and 10 (bottom spectra). The pH was adjusted by addition of concentrated NaOD or DCl to a 5 mM peptide solution in D_2O. In order to check the reproducibility of the results obtained at these pH values, samples were also prepared in 50 mM glycine buffer, pH 3, and in 50 mM CAPS buffer, pH 10. (A) Original spectra. (B) Same spectra as in (A) after Fourier self-deconvolution with a Lorentzian band of 12-cm^{-1} half-width and a band narrowing factor of 1.8.

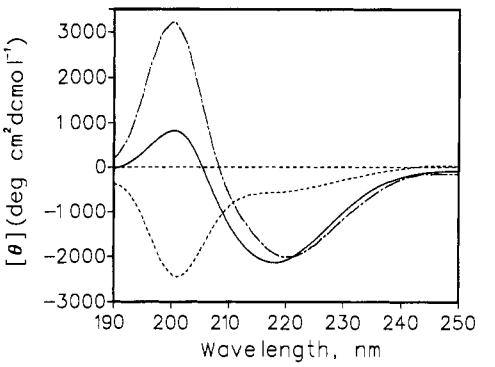

FIGURE 4: Circular dichroism spectra of peptide M (1.8 mM) as a function of pH. Peptide in 10 mM glycine buffer, pH 3 (—), in 10 mM HEPES buffer, pH 7 (- - -), and in 10 mM CAPS buffer, pH 10 (- · -).

The infrared spectra of peptide M in the intermediate pH range (4–9.5) are markedly different from those measured under highly basic conditions. As already briefly discussed (Figure 1), in this pH range the octadecapeptide adopts a predominantly β-sheet conformation, characterized by two strong infrared bands at 1612 and 1627 cm^{-1}. The β-sheet structure is also supported by the presence of a characteristic high-wavenumber component band at 1676 cm^{-1}. The minor bands between 1640 and 1665 cm^{-1} can be assigned to turns (1662 cm^{-1}), unordered segments (1642 cm^{-1}), and residual helix or turns (1652 cm^{-1}).

The infrared spectrum at low pH (below 4) reveals yet another conformation of peptide M. The original amide I band contour exhibits a very broad maximum centered at 1650 cm^{-1} and a weaker feature at 1612 cm^{-1} (Figure 3A, upper trace). The spectrum after band narrowing (Figure 3B) reveals the presence of two major bands at 1645 and 1659 cm^{-1}, with additional bands at 1612, 1627, and 1681 cm^{-1}. While the component at 1645 cm^{-1} represents nonordered peptide fragments, the conformational assignment of the component at 1659 cm^{-1} is debatable. Bands around 1660 cm^{-1} have been previously associated with distorted α-helices or with turns (Krimm & Bandekar, 1986). The weaker bands at 1612, 1627, and 1681 cm^{-1} indicate a residual β-structure. The broad bands at 1711 and 1723 cm^{-1} are due to the protonated carboxylate groups of glutamic acid and aspartic acid, respectively.

The dissimilar conformational preference of peptide M at different pH is also evident from the circular dichroism spectra shown in Figure 4. The results of circular dichroism (CD) experiments are generally consistent with the conformational assignments obtained from infrared spectroscopic analysis, although a direct comparison of the data is somewhat hampered by the different peptide concentrations used in the infrared and CD experiments. The CD spectrum of peptide M at pH 10 shows a pronounced minimum at approximately 200 nm and is fully characteristic of peptide chains in a nonordered conformation (Chang et al., 1978). The spectrum at neutral pH exhibits a minimum at 218 nm, a feature typical for polypeptides and proteins in a β-sheet conformation. The presence of some β-structure is also suggested by the CD spectrum of peptide M at pH 3. However, the latter spectrum is clearly not identical with that measured at pH 7, particularly with respect to the magnitude of the maximum around 200 nm.

The spectroscopic data clearly indicate that the conformation of peptide M in aqueous solution can be effectively controlled by the pH. Of particular interest is the structure adopted by the peptide in the intermediate pH range (4–9.5). The infrared spectra measured under such conditions are characterized by a strong low-wavenumber "β-band" at 1612 cm^{-1} which, as discussed above, denotes the presence of a network of hydrogen-bonded intermolecular β-sheets. The formation of peptide aggregates is also indicated by a relatively high turbidity of the peptide solution in the pH range 4–9.5. The disappearance (or a substantial reduction) of the 1612-cm^{-1} band at pH values above 9.5 and below 4 is accompanied by a rapid decrease in the turbidity of the sample, which becomes optically transparent.

The pH dependence of the self-association (formation of intermolecular β-sheets) points to the importance of electrostatic interactions in peptide M. The octadecapeptide contains two basic residues (lysine and arginine) and three acidic residues (glutamic acid and two aspartic acid residues). In the pH range between 4 and 9.5, all these residues are predominantly ionized. It may be thus postulated that the attractive electrostatic interaction (creation of "salt bridges") between the neighboring peptide molecules provides a driving force for the formation of intermolecular β-sheets. Neutralization of either acidic (low pH) or basic residues (high pH) leads to the disruption of these intermolecular associations.

The crucial role of electrostatic interactions is further supported by careful inspection of the bands representing vibrations of carboxylate groups of glutamic acid (1565 cm^{-1}) and aspartic acid (1586 cm^{-1}). At pH >4.5, these side-chain groups are essentially fully ionized. However, the carboxylate bands in the spectra measured in the pH range 4.5–9.5 are considerably broader and less intense than those in the spectra recorded at pH >9.5. This may be rationalized by the formation, at pH values between 4.5 and 9.5, of intermolecular salt bridges between carboxylate moieties and the basic residues (Mauk et al., 1986; Holloway & Mantsch, 1988).

Effect of Concentration on the Secondary Structure of Peptide M. Figure 5 shows infrared spectra of peptide M at neutral pH at four different concentrations between 0.5 and 5 mM. While the spectra remain practically unchanged at peptide concentrations above 2.5 mM, incremental dilution of the peptide solution from 2.5 to 0.5 mM results in a dramatic decrease in the intensity of the band at 1612 cm^{-1}, concomitant with an increase in the intensity of bands in the spectral region 1630–1660 cm^{-1}. Such a concentration de-

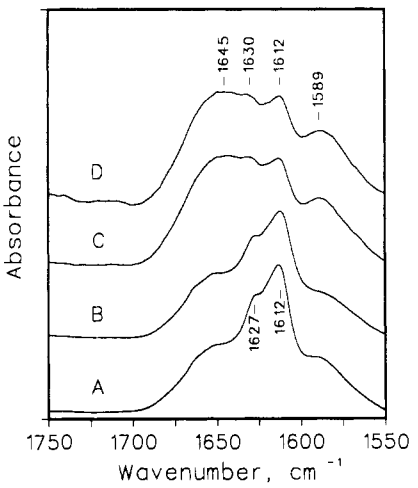

FIGURE 5: Infrared spectra of peptide M in the 1550–1750-cm^{-1} region as a function of concentration. The peptide was dissolved in 50 mM HEPES buffer, pH 7.0, at concentrations of 5 (A), 2.5 (B), 1 (C), and 0.5 mM (D).

pendence of the infrared spectra does support our assignment of the band at 1612 cm^{-1} to an intermolecular β-structure. A lowering of the concentration is likely to weaken the intermolecular interactions of the peptide, thus leading to a (at least partial) dissociation of the intermolecular β-sheets.

A concentration-dependent self-association that results in a more ordered secondary structure was previously reported for a number of short and intermediate-length peptides (Talbot et al., 1979; Gratzer & Beaver, 1969; Lau et al., 1983). However, while the prevailing structure in some other peptide aggregates is α-helix, the particular type of interactions in peptide M favors the formation of intermolecular β-sheets (or β-strands). From the pH dependence of infrared spectra (see above), we inferred that these sheets (strands) are stabilized by electrostatic interactions between the negatively charged carboxylate groups of aspartic acid and/or glutamic acid and the positively charged groups of arginine and/or lysine. This conclusion is further corroborated by the observation that the decrease in intermolecular β-sheet structure upon peptide dilution (as evidenced by a drop in the intensity of the 1612-cm^{-1} band) is accompanied by an increase in intensity of the bands below 1600 cm^{-1} which represent "free" carboxylate groups. The apparent "quenching" of the latter bands in the spectra of peptide M at high concentration points to the formation of salt bridges between carboxylate groups and basic residues of the neighboring peptide molecules.

While the concentration dependence of infrared spectra clearly demonstrates the relationship between the β-structure, expressed by the 1612-cm^{-1} band, and the degree of peptide self-association, it should be pointed out that the 1612-cm^{-1} band is still present (though considerably reduced) in the spectrum recorded at a peptide concentration as low as 1 mg/mL. Moreover, the latter spectrum also exhibits another β-band at 1630 cm^{-1}. Thus, even in a relatively dilute solution the peptide retains a considerable proportion of β-structure.

The concentration dependence of the conformation of peptide M is also evident from circular dichroism spectra, as shown in Figure 6. The CD spectrum measured at high peptide concentration (1.8 mM) shows a minimum at 218 nm and a weaker maximum at 200 nm, i.e., the features characteristic of β-sheet structures. The spectrum recorded at low peptide concentration (0.4 mM), in addition to a minimum at 218 nm, exhibits another minimum at around 200 nm; the spectral features at this low concentration are indicative of a mixture of β-structure and unordered conformation.

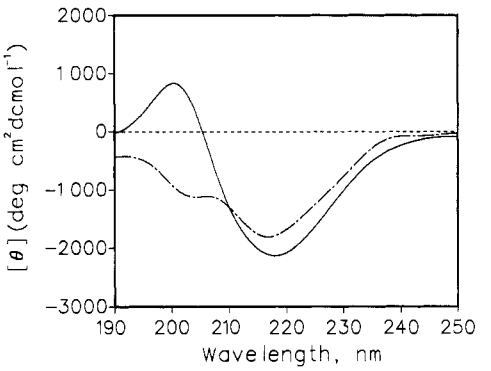

FIGURE 6: Circular dichroism spectra of peptide M in 10 mM Hepes buffer, pH 7.0, at concentrations of 1.8 (—) and 0.4 mM (- - -).

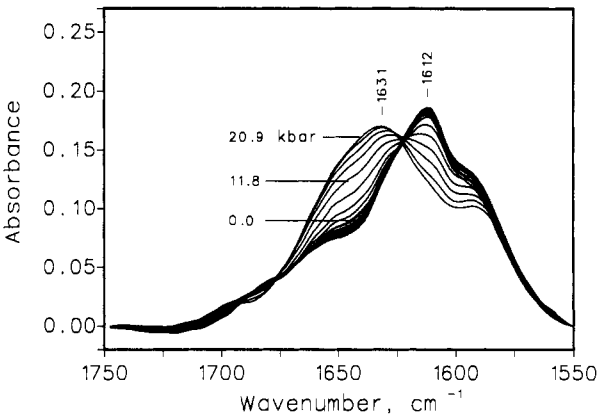

FIGURE 7: Infrared spectra of peptide M as a function of increasing hydrostatic pressure (up to 21 kbar). The peptide solution was prepared in 10 mM HEPES buffer, pH 7.0, at a concentration of 5 mM.

Effect of Pressure on the Secondary Structure of Peptide M. Elevated hydrostatic pressure is known to promote the dissociation of protein aggregates, particularly when these aggregates are stabilized by ionic interactions (Weber, 1987). Therefore, in order to gain additional insight into the conformation of peptide M under conditions favoring the monomeric state, the infrared spectrum of peptide M was further studied as a function of hydrostatic pressure.

As shown in Figure 7, the conformation-sensitive amide I bands of peptide M undergo substantial alterations in the pressure range approximately between 6 and 18 kbar. These changes are characterized by an increase in intensity of the bands in the region 1625–1665 cm^{-1}, which occurs at the expense of the initially dominating band at 1612 cm^{-1}. The gradual character of the pressure-induced spectral changes most likely reflects the fact that the equilibrium established at different pressures involves average forms of the aggregate and the monomers. Indeed, the existence of an equilibrium between two conformational states, one with the amide I maximum at 1612 cm^{-1} representing the aggregated peptide (oligomer) and a second one with the amide I maximum at 1631 cm^{-1} representing the fully dissociated peptide (monomer), is strongly supported by the appearance of an isosbestic point at 1622 cm^{-1} (Figure 7).

A convenient parameter to assess the pressure-induced changes in the infrared spectra of peptide M is the intensity ratio of the infrared bands at 1612 and 1631 cm^{-1}. As shown in Figure 8, the change in the intensity ratio I_{1612}/I_{1631} with pressure is dependent upon the peptide concentration; i.e., the midpoint of the spectral changes shifts toward higher pressure when the concentration of the peptide increases. This concentration dependence of the pressure effect further supports

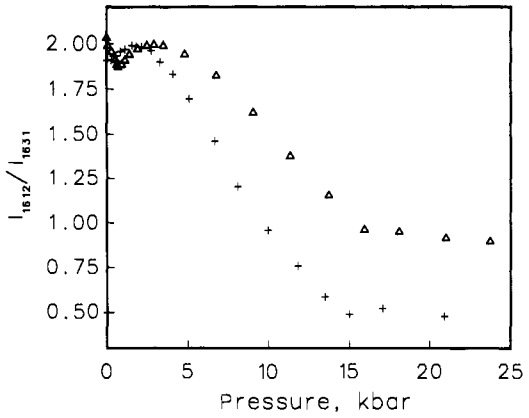

FIGURE 8: Pressure dependence of the peak height ratio I_{1612}/I_{1631} in the infrared spectra of peptide M in 10 mM HEPES buffer, pH 7.0, at concentrations of 10 (triangles) and 5 mM (crosses). Spectra were measured after incremental increases in pressure.

the notion that the spectral changes observed at high pressure are caused primarily by the dissociation of peptide aggregates and not by other factors (Silva et al., 1986).

The high-pressure spectrum with its maximum at 1631 cm^{-1} indicates that, at least at elevated pressure, the monomeric peptide adopts a predominantly β-structure. The conformation of the monomer at atmospheric pressure is more difficult to ascertain as under such conditions the equilibrium tends to be shifted toward the self-associated state of the peptide. Nevertheless, it is notable that a band at 1631 cm^{-1}, although not dominant, is also present in the spectrum recorded at atmospheric pressure and at the lowest measurable concentration of the peptide. Thus, the tendency of the monomeric peptide to fold into a β-structure seems to be evident already under ambient conditions; this conformational preference is further enhanced by an elevated pressure.

Concluding Remarks

Small polypeptides of less than 30 amino acids are generally believed to be highly flexible, capable of interconverting between a variety of different (usually loosely folded) conformations, depending on the solvent, pH, concentration, and the presence of other molecules in solution (Blundell & Wood, 1982). The conformational adaptability to environmental conditions has also been observed for the 18-residue peptide M. The remarkable feature of peptide M in the physiologically important pH range 4.5–9 is the ability to self-associate and to form a network of strongly hydrogen-bonded β-sheets. Although this tendency to self-associate prevents the precise determination of the secondary structure of the peptide in a monomeric state, both the concentration dependence and the pressure dependence of infrared spectra point to an at least partly folded conformation of the monomer, with a considerable proportion of β-structure. Our spectroscopic data are thus consistent with recently published theoretical predictions (Shinohara et al., 1987), which clearly favor an extended β-sheet for fragment 303–320 of the S-antigen (the amino acid sequence corresponding to peptide M).

In general, antigens are recognized by the B- and T-lymphocytes of the immune system. The B- and T-lymphocytes have many features in common, but the recognition of antigens by the two lymphocytes is quite different. The B-lymphocytes recognize the antigens in their native conformation, while the T-lymphocytes respond to a protein after it has undergone a process of degradation and has been cleaved into small peptide fragments. These small peptides are presented in association with the products of the major histocompatibility complex (MHC) on the surface of antigen-presenting cells. Therefore, the T-cell recognition of antigen requires the formation of a trimolecular complex consisting of a class I or class II MHC molecule, the peptide antigen, and the T-cell antigen receptor. The conformation of the peptide antigen is thus of primary importance in the MHC-restricted antigen recognition.

In this study, we have determined the conformational preferences of peptide M in aqueous solution. Due caution should be exercised in extrapolating the results of relatively simple physicochemical measurements in aqueous buffers to physiologically relevant situations in vivo. Nevertheless, the demonstrated propensity to form either an intermolecular (in the self-associated peptide) or an intramolecular (in a monomeric peptide) β-structure is likely to play a role in determining the immunogenic properties of peptide M. In this context, at least two different concepts have been put forward in an attempt to delineate the molecular basis for antigen recognition by T-helper cells. One model (De Lisi & Berzofsky, 1985; Pincus et al., 1983) proposes that antigenic sites on proteins consist of amphipathic α-helices, i.e., structures in which the hydrophobic and hydrophilic residues are separated on opposite faces of the helix. One face of the helix would be involved in the interaction with the presenting cell, whereas the other surface would confer specificity to the interaction with the T-cell receptor. An alternative model, proposed more recently by Sette et al. (1987), assumes that the immunogenic peptide adopts a planar conformation such that each of the residues is in a position to interact both with MHC and the T-cell receptor. A β-sheet structure consistent with the latter model has been found to be the most likely conformation of the immunogenic peptide from chicken ovalbumin, Ova 323–339, in its interaction with MHC (Sette et al., 1987). The conformational preferences of peptide M established in the present investigation provide another example of an immunogenic peptide that forms an extended β-structure. It is thus plausible that peptide M is recognized by a general mechanism similar to that suggested by Sette et al. (1987).

References

Blundell, T., & Wood, S. (1982) *Annu. Rev. Biochem. 51*, 123–154.

Byler, D. M., & Susi, H. (1986) *Biopolymers 25*, 469–487.

Carrier, D., Mantsch, H. H., & Wong, P. T. T. (1990) *Biopolymers* (in press).

Chang, C. T., Wu, C.-S. C., & Yang, J. T. (1978) *Anal. Biochem. 91*, 13–31.

Chirgadze, Y. N., Fedorov, O. V., & Trushina, N. P. (1975) *Biopolymers 14*, 679–694.

De Lisi, C., & Berzofsky, J. A. (1985) *Proc. Natl. Acad. Sci. U.S.A. 82*, 7048–7052.

Donoso, L. A., Merryman, C. F., Shinohara, T., Sery, T. W., & Smith, A. (1987) *Arch. Ophthalmol. 105*, 838–840.

Donoso, L. A., Yue, S., Sery, T. W., Merryman, C. F., Singh, V. K., & Shinohara, T. (1988) in *Molecular Biology of the Eye: Genes, Vision and Ocular Disease* (Piatigorsky, J., Shinohara, T., & Zelenka, P. S., Eds.) pp 385–398, Alan Liss, New York.

Gratzer, W. B., & Beaver, G. H. (1969) *J. Biol. Chem. 244*, 6675–6679.

Holloway, P. W., & Mantsch, H. H. (1988) *Biochemistry 27*, 7991–7993.

Kauppinen, J., Moffatt, D. J., Mantsch, H. H., & Cameron, D. G. (1981) *Appl. Spectrosc. 35*, 271–276.

Knight, M., Strickler, M. P., Stone, J., Chiodetti, L., Gluck, S., & Shinohara, T. (1988) *J. Chromatogr. 3*, 177–187.

Krimm, S., & Bandekar, J. (1986) *Adv. Protein Chem. 38*, 181-364.
Lau, S. H., River, J., Vale, W., Kaiser, E. T., & Kézdy, F. J. (1983) *Proc. Natl. Acad. Sci. U.S.A. 80*, 7070-7074.
Mantsch, H. H., Casal, H. L., & Jones, R. N. (1986) in *Spectroscopy of Biological Systems* (Clark, R. J. H., & Hester, R. N., Eds.) pp 1-46, Wiley, New York.
Mauk, M. R., Mauk, A. G., Weber, P. C., & Matthew, J. B. (1986) *Biochemistry 25*, 7085-7091.
Mochizuki, M., Kuwabara, T., McAllister, C., Nussenblatt, R. B., & Gery, I. (1985) *Invest. Ophthalmol. Visual Sci. 17*, 774-783.
Moffatt, D. J., Kauppinen, J. K., Cameron, D. G., Mantsch, H. H., & Jones, R. N. (1986) *Computer Programs for Infrared Spectrophotometry*, NRC Bulletin No. 18, NRC, Ottawa, Canada.
Parker, F. S. (1983) *Applications of Infrared, Raman and Resonance Raman Spectroscopy in Biochemistry*, Plenum Press, New York.
Pfister, C., Chabre, H., Plonet, J., Tuyen, V. V., Dekozak, Y., Faure, J.-P., & Kuhn, H. (1985) *Science 228*, 891-893.
Pincus, M. R., Gerewitz, F., Schwartz, R., & Scheraga, H. (1983) *Proc. Natl. Acad. Sci. U.S.A. 80*, 3297-3300.
Sette, A., Buns, S., Colon, S., Smith, J. A., Miles, C., & Grey, H. M. (1987) *Nature 328*, 395-399.
Shinohara, T., Dietzschold, B., Craft, C. M., Wistow, G., Early, J. J., Donoso, L. A., Horwitz, J., & Tao, R. (1987) *Proc. Natl. Acad. Sci. U.S.A. 84*, 6975-6979.
Shinohara, T., Donoso, L. A., Tsuda, M., Yamaki, K., & Singh, V. K. (1988) *Prog. Retinal Res. 8*, 51-66.
Silva, J. L., Miles, E. W., & Weber, G. (1986) *Biochemistry 25*, 5780-5786.
Singh, V. K., Nussenblatt, R. B., Donoso, L. A., Yamaki, K., Chan, C.-C., & Shinohara, T. (1988) *Cell. Immunol. 115*, 413-419.
Surewicz, W. K., & Mantsch, H. H. (1988) *Biochim. Biophys. Acta 952*, 115-130.
Surewicz, W. K., & Mantsch, H. H. (1989) *J. Mol. Struct. 214*, 143-147.
Surewicz, W. K., Mantsch, H. H., Stahl, G. L., & Epand, R. M. (1987) *Proc. Natl. Acad. Sci. U.S.A. 84*, 7028-7031.
Susi, H. (1969) in *Structure and Stability of Biological Macromolecules* (Timasheff, S. N., & Fasman, D. G., Eds.) pp 575-663, Marcel Dekker, New York.
Talbot, J. C., Dufourcq, J., deBorg, J., Faucon, J. F., & Lussan, C. (1979) *FEBS Lett. 102*, 191-193.
Wacker, W. B., Donoso, L. A., Kalsow, C. M., Yankeelov, J. A., & Organisciak, D. T. (1977) *J. Immunol. 119*, 1949-1958.
Weber, G. (1987) in *High Pressure Chemistry and Biochemistry* (van Eldik, R., & Jones, J., Eds.) pp 401-420, Reidel, Dordrecht, The Netherlands.
Wong, P. T. T., Moffatt, D. J., & Baudais, F. L. (1985) *Appl. Spectrosc. 39*, 733-735.

Calcium-Induced Lipid Phase Separations and Interactions of Phosphatidylcholine/Anionic Phospholipid Vesicles. Fluorescence Studies Using Carbazole-Labeled and Brominated Phospholipids†

John R. Silvius
Department of Biochemistry, McGill University, Montréal, Québec, Canada H3G 1Y6
Received September 13, 1989; Revised Manuscript Received November 27, 1989

ABSTRACT: A novel method that uses a carbazole-labeled fluorescent phosphatidylcholine, which partitions preferentially into liquid-crystalline lipid domains, to monitor the kinetics and the extents of thermotropic and ionotropic lateral phase separations in vesicles combining brominated and nonbrominated phosphatidylcholines (PCs), phosphatidic acids (PAs), and phosphatidylserines (PSs) is described. The calcium-induced segregation of several nonbrominated PA species in liquid-crystalline brominated PC bilayers behaves as a well-defined lateral phase separation; the residual solubility of the PA component in the PC-rich phase in the presence of calcium can vary severalfold depending on the PA acyl chain composition. PC/PS mixtures show a pronounced tendency to form metastable solutions in the presence of calcium, particularly when they contain less than equimolar proportions of PS. This metastability is not readily relaxed by repeated freeze–thawing of vesicles in the presence of calcium, by avidin-mediated contacts between PC/PS vesicles containing biotinylated lipids, or by calcium-induced lateral segregation of PA in the same vesicles. Different PS species exhibit different apparent residual solubilities in liquid-crystalline PC bilayers, ranging from <10 mol % for dimyristoyl-PS to ca. 45 mol % for dioleoyl-PS, after prolonged incubations of PC/PS multilamellar vesicles with excess calcium. Results are presented, obtained by using the above lipid-segregation assay and parallel assays of intervesicle lipid mixing, that raise questions concerning the relevance of the equilibrium behavior of calcium-treated PS/PC mixtures to the relatively rapid interactions (fusion and lipid mixing) of PC/PS vesicles that follow initial exposure to calcium.

Since most biological membranes contain a wide variety of different lipid species, an understanding of the interactions and the lateral distributions of different lipids in multicomponent bilayer membranes is important to understand many aspects of membrane behavior. Several physical techniques, including calorimetry, nuclear magnetic resonance, electron spin resonance, vibrational spectroscopy, X-ray diffraction, and

†This work was supported by grants from the Medical Research Council of Canada and les Fonds FCAR du Québec.

0006-2960/90/0429-2930$02.50/0